Electronic Supplementary Material (ESI) for Nanoscale.

Supporting Information

Hydrothermal synthesis of Pt-Ag alloy nanooctahedra and their enhanced electrocatalytic activity for the methanol oxidation reaction

Geng-Tao Fu,[b] Ru-Guang Ma,[c] Xue-Qing Gao,[a] Yu Chen,*[ab] Ya-Wen Tang,[b] Tian-Hong Lu,[b] and Jong-Min Lee*[c]

[a] School of Materials Science and Engineering, Shaanxi Normal University, Xi'an 710062, PR China

[b] Jiangsu Key Laboratory of New Power Batteries, Jiangsu Collaborative Innovation Center of Biomedical Functional Materials, Analysis and Testing Center, School of Chemistry and Materials Science, Nanjing Normal University, Nanjing 210023, PR China

[c] School of Chemical and Biomedical Engineering Nanyang Technological University, Singapore 637459, Singapore

Experimental section

Reagents and chemicals

Polyallylamine hydrochloride (PAH, weight-average molecular weight 15 0000) was supplied from Nitto Boseki Co., Ltd. (Tokyo, Japan). Silver nitrate ($AgNO_3$), potassium tetrachloroplatinate(II) (K_2PtCl_4) and formaldehyde solution (HCHO, 40%) were purchased from Sinopharm Chemical Reagent Co., Ltd (Shanghai, China). Commercial Pt black was purchased from Johnson Matthey Corporation. Other reagents were of analytical reagent grade and used without further purification.

Preparation of Pt-Ag alloy nanooctahedra

In a typical synthesis, 0.5 mL of 0.05 M K_2PtCl_4, 0.5 mL of 0.05 M $AgNO_3$ and 1.0 mL of 0.50 M PAH (molarity of PAH given with respect to the repeating unit) aqueous solutions were added into 7.5 mL of water with continued stirring (Noting: the interaction between Ag^+ and Cl^- generates AgCl precipitate during mixing). After adding a 0.5 mL of HCHO solution (40%), the resultant mixture (pH 3.0) was transferred to a 20-mL Teflon-lined stainless-steel autoclave, and was then heated at 180 °C for 4 h. After being cooled to room temperature, the obtained Pt-Ag alloy nanooctahedra were separated by centrifugation at 15000 rpm for 15 min, washed with acetic acid for 12 h to remove redundant PAH,[1, 2] and then dried at 60 °C for 5 h in a vacuum dryer. Under the same conditions, a series of controlled experiments were also conducted to investigate the formation/growth mechanisms of the Pt-Ag alloy nanooctahedra.

Electrochemical instrument

All electrochemical experiments were performed by using a CHI 660 C electrochemical analyzer (CH Instruments, Shanghai, Chenghua Co., Ltd.). A standard three-electrode system was used for all electrochemical experiments, which consisted of a platinum wire as the auxiliary electrode, a saturated calomel reference electrode (SCE) protected by Luggin capillary with KCl solution as the reference electrode, and a catalyst modified glassy carbon electrode as the working electrode.

Potentials in this study were reported with respect to SCE. All electrochemical measurements were carried out at 30 ±1 °C.

An evenly distributed suspension of catalyst was prepared by ultrasonic the mixture of 10 mg catalyst and 5 mL H_2O for 30 min, and 6 μL of the resulting suspension was drop-cast onto the surface of the glassy carbon electrode (3 mm diameter). After drying at room temperature, 3 μL of Nafion solution (5 wt. %) was covered on the modified electrode surface and allowed drying again. Thus, the working electrode was obtained, and the specific loading of metal on the electrode surface was about 170 μg cm^{-2}. Electrochemical measurements were conducted in N_2-saturated 0.5 M H_2SO_4 solution or N_2-saturated 0.5 M H_2SO_4 solution with 1.0 M CH_3OH.

Instruments

Transmission electron microscopy (TEM) images and energy-dispersive X-ray spectroscopy (EDX) elemental mapping patterns were taken using a JEOL JEM-2100F transmission electron microscopy operated at 200 kV. The samples were prepared by placing a drop of the colloidal solution or catalyst powder dispersion in ethanol solution (99%) on a carbon film coated Cu grid (3 mm, 300 mesh), followed by drying under ambient conditions. X-ray diffraction (XRD) patterns were obtained with a Model D/max-rC X-ray diffractometer using Cu Ka radiation source (λ=1.5406 Å) and operating at 40 kV and 100 mA. High-resolution X-ray photoelectron spectroscopy (XPS) was carried out on a Thermo VG Scientific ESCALAB 250 spectrometer with an Al Kα radiator, and the vacuum in the analysis chamber was maintained at about 10^{-9} mbar. The binding energy was calibrated by means of the C 1s peak energy of 284.6 eV.

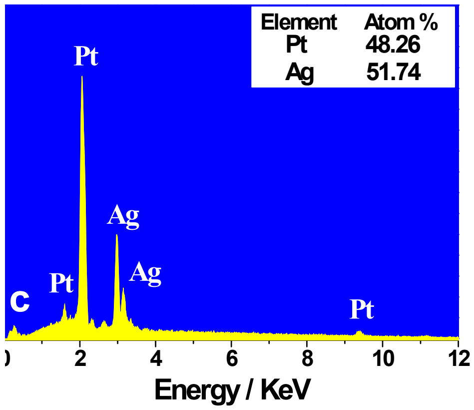

Fig. S1 EDX spectrum of the products

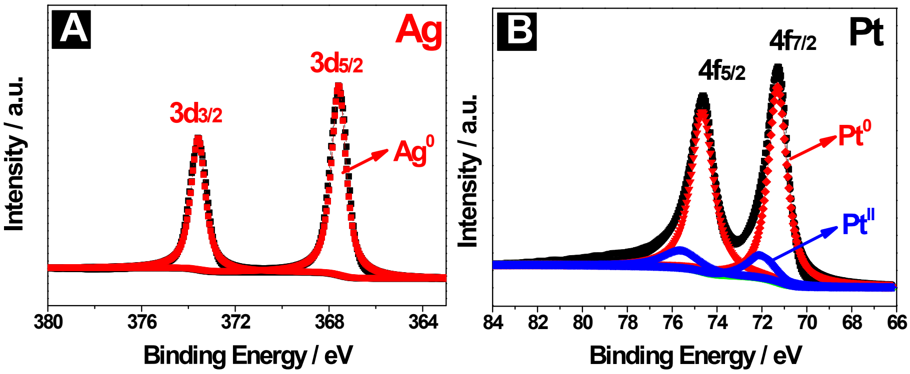

Fig. S2 XPS spectra of the products in the (A) Ag 3d and (B) Pt 4f regions.

XPS spectrum of Ag 3d displays two peaks at 367.60 eV (Ag 3d5/2) and 373.60 eV (Ag 3d3/2) with a spin-orbit separation of 6.0 eV, which is indicative of elemental Ag^0 (Figure S2A). XPS spectrum of Pt 4f displays two peaks at 71.26 eV (4f7/2) and 74.59 eV (4f5/2) with a spin-orbit separation of 3.35 eV (Figure S2B). The fitting curves show the percentage of Pt^0 species is 88.4% . Based on the integrated area and sensitivity factors of Pt 4f and Ag 3d, the surface atomic ratio of Pt and Ag atoms is calculated to be 49:51, consistent with the bulk composition obtained from EDX data, which is indicative of Pt-Ag alloy structure.

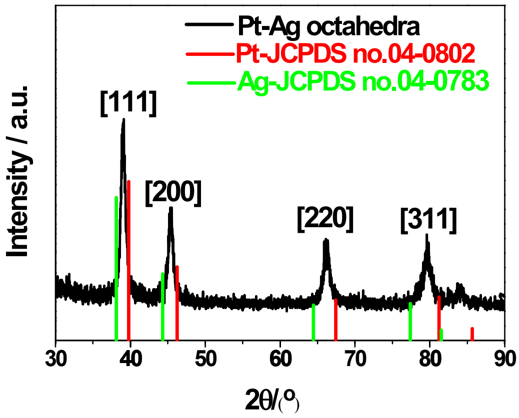

Fig. S3 XRD pattern of the Pt-Ag alloy nanooctahedra.

The crystal structure of the as-prepared Pt-Ag alloy nanooctahedra was characterized by XRD. The different diffraction peaks can be indexed to (111), (200), (220), and (311) facets, demonstrating that Pt-Ag alloy nanooctahedra can be identified as *fcc* structure. Meanwhile, all diffraction peaks of the Pt-Ag alloy nanooctahedra shift to a higher angle than the Ag element (JCPDS no.: 04-0783 Ag), and no diffraction peaks for single-component Pt and Ag are observed, indicating the products are phase pure. The average lattice parameter value (a) of the Pt-Ag nanooctahedra, calculated from the four different diffraction peaks, is 0.40060 nm (Table S1). This is smaller than that of bulk Ag (PDF#04-0783 Ag, a=0.40856 nm), reflecting the lattice contraction due to the partial substitution of Ag by Pt. Based on the Vegard's equation of $a = a_2\times[1+(a_1-a_2)/a_2\times x_1]$, the alloying Ag content in the Pt-Ag alloy nanooctahedra (with respect to Pt) is calculated to be 49 at.%, in consistent with the EDX composition (atomic ratio of Ag and Pt is 48:52), indicating that the the Pt-Ag nanooctahedra are indeed an alloy structure. Where a, a_1, and a_2 are lattice parameters for the Pt-Ag bimetallic alloy, pure Pt and pure Ag, respectively, and x_1 is the molar ratio of Ag in the bimetallic alloy.[3, 4]

Table S1. The lattice parameter (a) values of the Pt-Ag alloy nanooctahedra estimated from all XRD peaks.

Samples	**a**-{111}	**a**-{200}	**a**-{220}	**2**-{311}	**a**-Average
Octahedra	0.40081	0.40093	0.40050	0.40016	0.40060
Pure Pt	0.39225	0.39226	0.39220	0.39226	0.39224
Pure Ag	0.40857	0.40878	0.40863	0.40826	0.40856

$$a = \frac{\lambda}{2\sin\theta} \times \sqrt{h^2 + k^2 + l^2}$$

where λ is the wavelength of X-ray which equals to 1.5405 Å for Cu Ka source; θ the diffraction angle, and (*h, k, l*) the Miller indices.

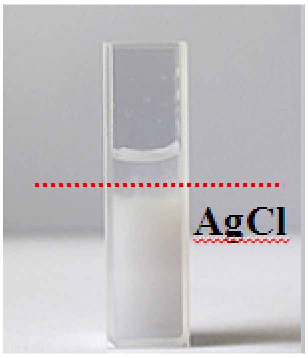

Fug. S4 Digital photograph of white AgCl precipitate after adding $AgNO_3$ into PAH solution.

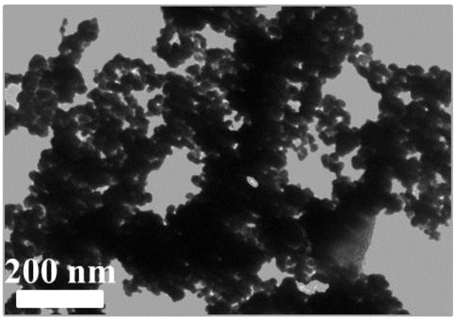

Fig. S5 TEM image of the products synthesized under the standard experimental condition except the exclusion of PAH.

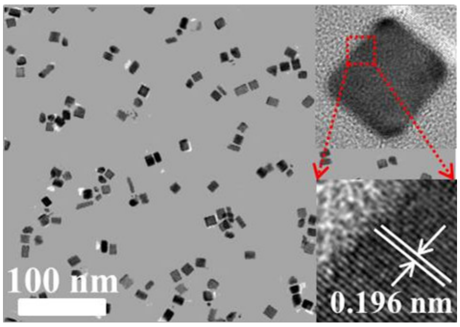

Fig. S6 TEM image of the Pt nanocubes synthesized under the standard experimental condition in the absence of $AgNO_3$.

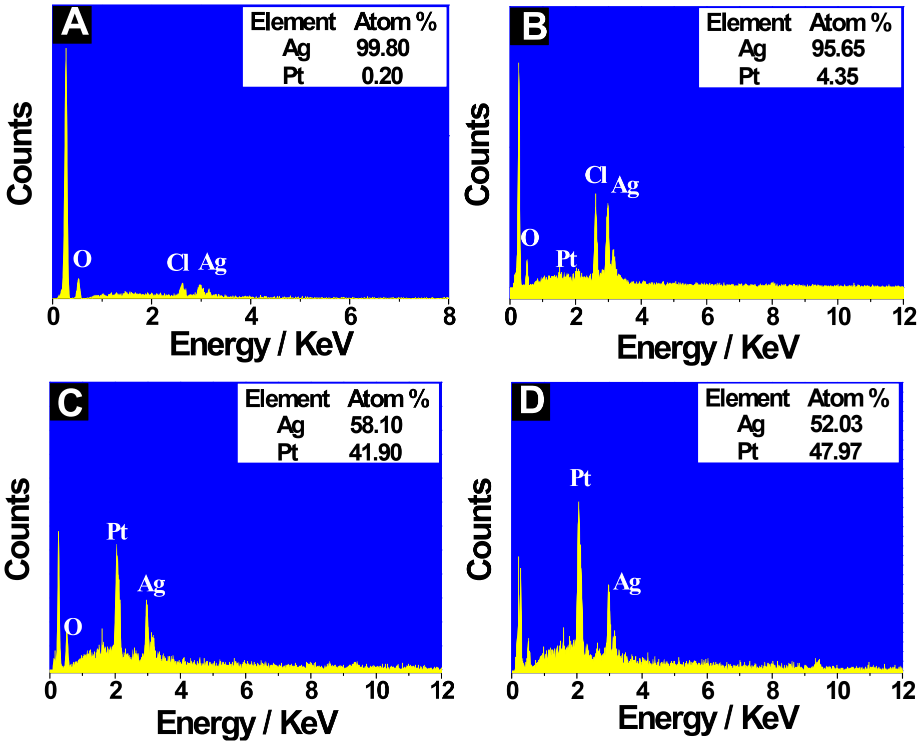

Fig. S7 EDX spectra of the intermediates collected at different growth stages: (A) 30 min, (B) 1 h, (C) 2 h, and (D) 4 h.

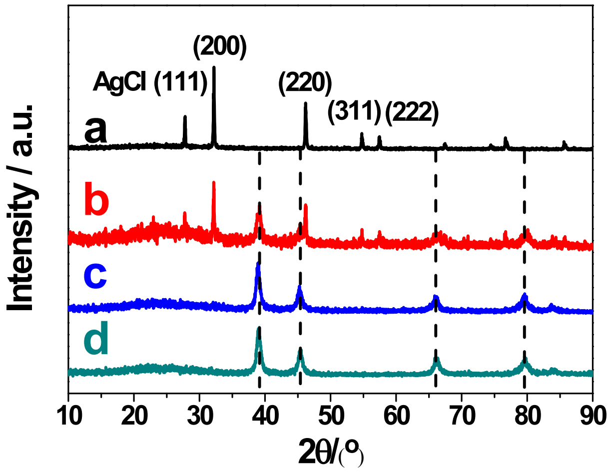

Fig. S8 XRD patterns of the intermediates collected at different growth stages: (a) 30 min, (b) 1 h, (c) 2 h, and (d) 4 h.

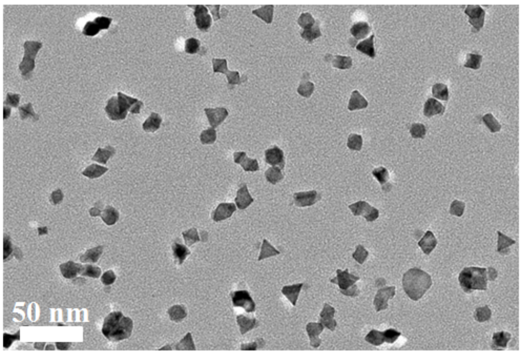

Fig. S9 TEM image of the Pt-Ag nanocrystals prepared by displacing the air with N_2 to eliminate typical etchant O_2 under standard experimental conditions.

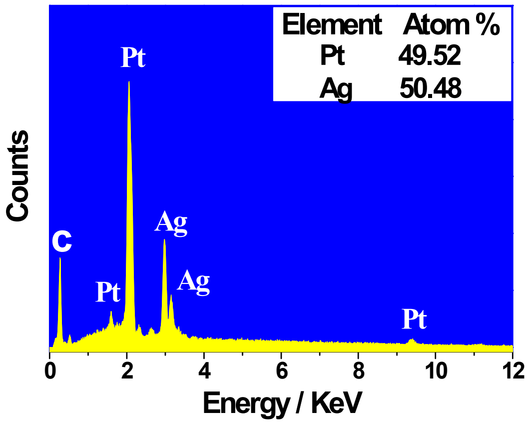

Fig. S10 EDX spectrum of the Pt-Ag alloy nanooctahedra an additional 50 cycles of electrochemical cleaning.

Reference

1. V. Mazumder and S. Sun, *J.Am. Chem. Soc.*, 2009, **131**, 4588-4589.
2. G. Fu, R. Zhao, L. Ding, L. Tao, J. Lin, Y. Chen, Y. Tang, Y. Zhou and T. Lu, *ChemPlusChem*, 2013, **78**, 623-627.
3. C. Bassett, R. Pawluk and A. Pilla, *Annals of the New York Academy of Sciences*, 1974, **238**, 242-262.
4. Z. Peng and H. Yang, *J. Solid State Chem.*, 2008, **181**, 1546-1551.